Synthesis and Characterization of Ti-HMS and CoMo/Ti-HMS Oxide Materials with Varying Ti Content

T. A. Zepeda,*[,†,‡] J. L. G. Fierro,[†] B. Pawelec,[†] R. Nava,[‡] T. Klimova,[§] G. A. Fuentes,[||] and T. Halachev[‡]

Instituto de Catálisis y Petroleoquímica, CSIC, c/Marie Curie 2, Cantoblanco, 28049 Madrid, Spain, Centro de Física Aplicada y Tecnología Avanzada-UNAM, Campus Juriquilla, Querétaro, A. P. 1-1010, 76230, México, Facultad de Química, UNAM, Cd. Universitaria, México, D.F. 04510, México, and Área de Ingeniería Química, Universidad A. Metropolitana-Iztapalapa, A.P. 55-534, 09340 México D.F., México

Received January 3, 2005. Revised Manuscript Received May 25, 2005

Hexagonal mesoporous materials with wormhole framework structures having Si/Ti molar ratios of 80, 40, and 20 (Ti-HMS) were used as supports of CoMo HDS catalysts. The supports and catalysts were characterized by N_2 adsorption−desorption (S_{BET}), X-ray diffraction (XRD), UV−vis diffuse reflectance spectroscopy (DRS UV−vis), X-ray photoelectron spectroscopy (XPS), ^{29}Si nuclear magnetic resonance (^{29}Si NMR), FT-IR of adsorbed NO, and reactivity. The catalysts were tested in the reaction of hydrodesulfurization (HDS) of dibenzothiophene (DBT). The incorporation of titanium into the framework of HMS did not change its mesoporous character but modified the surface properties. The presence of Ti impedes the formation of Co_2SiO_4 and of β-$CoMoO_4$ phases and increases the amount of octahedral Co species. The incorporation of titanium into the HMS framework led to an increase in the catalytic activity in comparison to that of the Ti-free catalyst. All Ti-containing catalysts manifest higher activity than that of a conventional $CoMo/Al_2O_3$ catalyst. The effect of Ti is not linear, the highest activity was observed for the sample with Si/Ti = 40 atomic ratio. This catalyst demonstrated to be 30% more active than the conventional industrial catalyst and 50% more active than the Ti-free catalyst. It is suggested that the higher activity of this catalyst is related to the higher value of the Co/Mo ratio in the sulfide state of the catalysts, to the larger amount of exposed Co species and to the specific degree of sulfidation of the Co species, characterized by specific electronic properties, which promote both the DDS and the HYD routes of HDS of DBT. The large pore diameter of this sample should also contribute to the elimination of possible diffusion effects.

1. Introduction

Hydrodesulfurization (HDS) of petroleum fractions is one of the most important processes in the refining industry due to the ever increasing amounts of heavier feeds and the severe restrictions imposed on the allowed percentage of sulfur- and nitrogen-containing compounds as well as of aromatics in the distillate fractions.[1] The demand for lower content of sulfur in the fuels requires the synthesis of more active HDS catalysts.[2,3] One of the major factors that affect the activity of the HDS catalyst is the interaction between the active components of the catalyst and the support. Molybdenum-based hydroprocessing catalysts are usually supported on γ-Al_2O_3.[4] There have been a number of studies on support effects in HDS and related reactions using a variety of supports such as γ-Al_2O_3,[5,6] $SiO_2-Al_2O_3$,[7−9] ZrO_2,[10,11] and mixed oxides such as TiO_2-ZrO_2,[12] $TiO_2-Al_2O_3$,[13−15] and TiO_2-SiO_2.[13,14] Suitable carrier for this purpose could be also the recently synthesized MCM-41 material.[16] This material resulted to be an excellent support for preparation of bifunctional catalysts.[17] Another mesoporous material, the hexagonal mesoporous silica (HMS), prepared by a neutral templating pathway[18] offers certain advantages over the

* Corresponding author. Tel.: +(52)5556234163. Fax: +(52)5556234165. E-mail: trino@icp.csic.es.
[†] CSIC.
[‡] Centro de Física Aplicada y Tecnología Avanzada-UNAM.
[§] UNAM.
[||] Universidad A. Metropolitana-Iztapalapa.

(1) Eastwood, D.; Van de Venne, H. Presented at the NPRA Annual Meeting, San Antonio, TX, March 1990.
(2) Topsøe, H.; Clausen, B. S.; Massoth F. E. In *Hydrotreating Catalysts: Science and Technology*; Springer: Berlin, 1996; p 310.
(3) Whitehurst, D. D.; Isoda, T.; Mochida. I. *Adv. Catal.* **1998**, *42*, 345.
(4) Knudsen, K. G.; Cooper, B. H.; Topsøe. H. *Appl. Catal. A* **1999**, *189*, 205.
(5) Murali Dhar, G.; Ramakrishna, H.; Prasada Rao, T. S. R. *Catal. Lett.* **1993**, *22*, 351.
(6) Okamoto, Y.; Maezawa, A.; Imanaka, T. *J. Catal.* **1989**, *120*, 29.
(7) Rao, K. S. P.; Murali Dhar, G. *J. Catal.* **1989**, *115*, 227.
(8) Massoth, F. E.; Murali Dhar, G.; Shabtai. J. *J. Catal.* **1994**, *85*, 44.
(9) Massoth, F. E.; Murali Dhar, G.; Shabtai. J. *J. Catal.* **1994**, *85*, 52.
(10) Rao, K. S. P.; Ramakrishna, H.; Murali Dhar. G. *J. Catal.* **1992**, *133*, 146.
(11) Vrinat, M.; Hamon, D.; Breysse, M.; Durand, B. *Catal. Today* **1994**, *20*, 273.
(12) Daly, F. P.; Ando, H.; Schmitt, J. L.; Sturm. E. A. *J. Catal.* **1987**, *108*, 401.
(13) Zhaobin, W.; Qin, X.; Xiexian, G.; Sham, E. L.; Grange, P.; Delmon, B. *Appl. Catal.* **1990**, *63*, 305.
(14) Zhaobin, W.; Qin, X.; Xiexian, G.; Sham, E. L.; Grange, P.; Delmon, B. *Appl. Catal.* **1991**, *75*, 179.
(15) Pophal, C.; Kameda, F.; Hoshino, K., Yoshinaka, S.; Segawa, K. *Catal. Today* **1997**, *39*, 21.
(16) Kresge, C. T.; Leonowich, M. E.; Roth, W. J.; Vartuli, J. C.; Beck, J. S. *Nature* **1992**, *359*, 710.
(17) Corma, A. *Chem. Rev.* **1995**, *95*, 559.
(18) Tanev, P. T.; Pinnavaia, T. *Science* **1995**, *267*, 865.

10.1021/cm0500051 CCC: $30.25
Published on Web 07/12/2005

electrostatically templated MCM-41 material. HMS materials (substituted by Al, Ti, Zr, etc.) have been reported to be more active in the HDS of DBT in comparison to the MCM-41 supports.[19] The differences observed in the catalytic activity can be due to the difference in the textural properties. Halachev et al.[20] reported higher catalytic activity of a NiW/(P)Ti-HMS catalyst in hydrogenation of naphthalene in comparison to a conventional alumina-supported catalyst. Chiranjeevi et al.[21] used HMS, Al-HMS, and γ-Al_2O_3 materials as supports in the preparation of W, CoW, and NiW catalysts, with W-loading varying from 10 to 25 wt %, and the promoter concentration (Co or Ni) was of 3 wt %. The promotional effects were studied over catalysts containing W-loadings of 21 wt %. The catalysts were tested in the HDS of thiophene and the hydrogenation of cyclohexene. The catalysts supported on HMS and Al-HMS materials showed higher catalytic activities in comparison to the catalyst supported on γ-Al_2O_3. Later, the same authors[22] used HMS, Al-HMS, and γ-Al_2O_3 materials as supports of Mo, CoMo, and NiMo catalysts in the same reactions. The promoter concentration was of 3 wt % of Co or Ni. The promotional effects were studied on 10 wt % Mo. A better catalytic activity for the CoMo/Al-HMS catalyst was observed in the HDS of thiophene, and the highest catalytic activity in the hydrogenation of cyclohexene was observed over the NiMo/Al-HMS catalyst. Our preliminary results[23] showed that a CoMo/Ti-HMS (3.2 wt % of TiO_2) catalyst manifests higher activity in the HDS of DBT in comparison to a CoMo/HMS and a conventional alumina-supported catalyst.

The excellent performance in HDS and hydrogenation reactions displayed by HMS substrates, containing heteroatoms incorporated in its framework, has been related to the high specific area, large pore size, and large pore volume. Since the Ti-HMS support has favorable textural parameters, it is an excellent candidate to be used as a support for CoMo catalysts. To date, the application of the Ti-HMS materials as supports of CoMo hydrotreating catalysts has not been reported.

In the present work, HMS and Ti-HMS materials with varying titanium content (Si/Ti atomic ratios of 80, 40, and 20) were synthesized and used for the preparation of CoMo catalysts. The catalysts were tested in the reaction of HDS of DBT. The supports and catalysts were characterized by N_2 adsorption−desorption (S_{BET}), X-ray diffraction (XRD), UV−vis diffuse reflectance spectroscopy (DRS UV−vis), X-ray photoelectron spectroscopy (XPS), ^{29}Si nuclear magnetic resonance (^{29}Si NMR), and FT-IR of adsorbed NO.

Table 1. Chemical Composition of the Catalysts

sample	Mo (wt %)[a]	Co (wt %)[a]
CoMo/HMS	9.0	3.0
CoMo/Ti-HMS-80	9.0	3.0
CoMo/Ti-HMS-40	9.0	3.0
CoMo/Ti-HMS-20	9.0	3.0
industrial	12	3.9

[a] Nominal composition.

2. Experimental Section

2.1. Synthesis of the HMS and Ti-HMS Materials. HMS was synthesized by the neutral S^0I^0 templating route, proposed by Tanev and co-workers,[18,24] which is based on hydrogen bonding and self-assembly between neutral primary amine surfactants (S^0) and a neutral inorganic precursor (I^0). The Ti-HMS material was prepared following a procedure similar to that described by Gotier and Tuel[25] using dodecylamine ($C_{12}H_{25}NH_2$, Aldrich 98%) as surfactant, but the reaction mixture was slightly modified by the addition of the swelling agent mesitylene (C_9H_{12}, Aldrich 98%), as first proposed by Kresge et al.[16] The Ti-HMS material was synthesized with Si/Ti molar ratios equal to 20, 40, and 80. The reaction products were filtered, washed with distilled water, and dried at room temperature for 24 h, followed by drying at 378 K for 2 h. Subsequently, the samples were calcined at 823 K for 3.5 h in air, with a heating rate of 2.5 K/min.

2.2. Catalysts Preparation. The catalysts were prepared by successive impregnation using the pore-filling method. Molybdenum was introduced first from an aqueous solution of ammonium heptamolybdate ($(NH_4)_6Mo_7O_{24}$, Aldrich 99%). The obtained samples were dried at room temperature for 18 h and then at 378 K for 2 h. Then the samples were calcined at 773 K for 4.5 h, reaching this temperature within 3.5 h. Then the solution with the corresponding concentration of cobalt nitrate ($Co(NO_3)_2$, Aldrich 98%) was added. Subsequently, the samples were dried at room temperature for 18 h and then at 378 K for 2 h followed by calcination at a 773 K for 4.5 h, reaching this temperature within 3.5 h. The chemical composition and denomination of the catalysts is given in Table 1. One of the most important questions in the preparation of these catalysts is up to what extent are the Ti ions incorporated into the framework of the supports and if segregation of TiO_2 takes place on their surface. This problem is of crucial importance in elucidating the effect of the Ti ions on the catalytic properties of these materials.

2.3. Sulfidation of the Catalysts. The catalysts were sulfided in a U-shape glass flow reactor. First the sample was flushed in a nitrogen flow gradually increasing the temperature up to 423 K and then switching to the sulfidation mixture (H_2/H_2S 10 vol % H_2S) at a flow of 60 mL min^{-1} and increasing the temperature up to 673 K, reaching this temperature within 2.5 h. The sulfidation was carried out at this temperature for 2 h. Then the sample was cooled to room temperature, changing the sulfidation mixture to nitrogen when the temperature had decreased to 423 K. The sulfided sample was transferred to the reactor in an argon atmosphere with the aim to avoid contact with air.

2.4. Characterization Methods. 2.4.1. N_2 Adsorption−Desorption Isotherms. The nitrogen adsorption−desorption isotherms were determined on a ASAP 2000 Micromeritics equipment. Prior to the experiments, the samples were degassed at 543 K in a vacuum for 5 h. The volume of the adsorbed N_2 was normalized to the standard temperature and pressure. Specific surface area (S_{BET}) was calculated by the BET equation applied to the range of relative

(19) Segawa, K.; Santo, S. In *Hydrotreatment and Hydrocracking of Oil Fractions*; Delmon, B. F., Froment, G. F., Grange, P., Eds.; Studies in Surface Science and Catalysis Vol. 127B; 1999; pp 127−129.
(20) Halachev, T.; Nava, R.; Dimitrov, L. D. *Appl. Catal. A* **1998**, *169*, 111.
(21) Chiranjeevi, T.; Kumar, P.; Maity, S. K.; Rana, M. S.; Murali Dhar, G.; Prasada Rao, T. S. R. *Microporous Mesoporous Mater*. **2001**, *44*, 547.
(22) Chiranjeevi, T.; Kumar, P.; Rana, M. S.; Murali Dhar, G.;. Prasada Rao, T. S. R. *J. Catal*. **2002**, *181*, 109.
(23) Zepeda, T.; Halachev, T.; Nava, R.; Pawelec, B.; Klimova, T.; Fuentes, G. A.; Fierro, J. L. G. Hydrodesulfurization of dibenzotiophene over CoMo/HMS and CoMo/Ti-HMS catalysts. Unpublished results.
(24) Tanev, P.; Chibwe, M.; Pinnavaia, T. J. *Nature* **1994**, *368*, 321.
(25) Gotier, S.; Tuel, A. *Zeolites* **1995**, *15*, 601.

pressures $0.05 < P/P^0 < 0.30$. The average pore diameter was calculated by applying the Barret−Joyner−Halenda method (BJH) to the adsorption branches of the N_2 isotherms. The cumulative pore volume was obtained from the isotherms at $P/P^0 = 0.99$.

2.4.2. X-ray Diffraction. The X-ray patterns were recorded on a Rigaku 2100 diffractometer, using a monochromatic Cu Kα radiation ($\lambda = 0.1541$ nm). The diffractograms were recorded in the 2θ range of 0.5−80° at a step of 0.02°.

2.4.3. UV−Vis Diffuse Reflectance Spectroscopy. The UV−vis diffuse reflectance spectra (DRS UV−vis) of the pure supports and the catalysts in their oxide state were recorded using a Cary 5_E spectrophotometer with a specially designed Praying Mantis diffuse reflection attachment (Harrick) for in situ measurements. All spectra were recorded after heating the samples at 523 K in He flow during 1 h. The spectrum of the corresponding support was subtracted from the spectrum of the catalyst. Decomposition of each spectrum was performed by nonlinear fitting of multiple Gaussian peak functions sharing a common baseline.

2.4.4. X-ray Photoelectron Spectroscopy (XPS). The X-ray photoelectron spectra of the supports and the sulfided catalysts were recorded with the aim to study the effect of Ti on the dispersion and the degree of sulfidation of the supported species. A VG Escalab 200R spectrometer equipped with a hemispherical electron analyzer and a Mg Kα ($h\nu = 1253.6$ eV) X-ray source was used. The samples were first placed in a copper holder mounted on a sample-rod in the pretreatment chamber of the spectrometer and then outgassed at 403 K for 1 h before transfer to the analysis chamber. The freshly sulfided CoMo catalysts were kept under isooctane in order to avoid exposure to air and then introduced to the preparation chamber. All supports and catalysts were outgassed at 10^{-5} mbar and then transferred to the ion-pumped analysis chamber, where residual pressure was kept below 7×10^{-9} mbar during data acquisition. The binding energies (BE) were referenced to the C 1s peak (284.9 eV) to account for the charging effects. The areas of the peaks were computed after fitting of the experimental spectra to Gaussian/Lorentzian curves and removal of the background (Shirley function). Surface atomic ratios were calculated from the peak area ratios normalized by the corresponding atomic sensitivity factors.[26]

2.4.5. Nuclear Magnetic Resonance (NMR). The NMR spectra were recorded on a Brucker AV 400 WB spectrometer with the aim to verify the incorporation of the Ti ions into the silica framework of the supports. The dried powdered samples were loaded into a BL4 X/Y/1H 4-mm multinuclear probe and spun at 5 kHz according to the following protocol: $\pi/2$ pulse, 7 μs; CP contact time 2 ms; 1700 scans. An internal reference of the spectrometer was employed to calculate the chemical shifts.

2.4.6. FT-IR Spectra of Adsorbed NO. The adsorption of NO was used to measure the dispersion of the supported metal species. Self-supporting wafers of the catalysts with thickness of 12 mg cm^{-2} were prepared by pressing the powdered samples at a pressure of 7×10^3 kg cm^{-2} during 10 min. The samples were degassed at 673 K for 2 h in a special IR cell having greaseless stopcocks and KBr windows. Once the samples were cooled to ambient temperature, they were exposed to 20 mbar of NO during 5 min. Subsequently, the spectrum was recorded on a Nicolet 510 FTIR spectrophotometer at a resolution of 4 cm^{-1}. Then the sample was degassed at 673 K during 2 h to achieve total desorption of the NO molecules, and the spectrum of the catalyst was recorded. The IR spectrum of the adsorbed NO was obtained by subtracting the spectrum of the corresponding, degassed at 673 K catalyst.

2.4.7. Catalytic Activity Measurements. The catalytic activity in the reaction of HDS of DBT was measured in a batch Parr reactor charged with 0.2 g of the catalyst and 0.3 g of DBT dissolved in 100 mL of *n*-hexadecane. The reactor was additionally purged with nitrogen to eliminate traces of oxygen. The reaction was carried out for 6 h at 593 K under hydrogen pressure of 5.5 MPa. The stirring of the reaction mixture was sufficiently intensive to exclude external diffusion limitations (checked by varing amount of catalyst and the power of stirring (1000, 800, and 700 rpm). To minimize internal diffusion limitations, all catalysts were thoroughly ground to a fine powder. The heat-up time of the reactor to the reaction temperature was 35 min. The reaction products were analyzed by GC on a Perkin-Elmer XL equipment using a 30 m long Altech econo capillary column. The mass balance in all experiments was within the 99.0−99.98% range. The degree of conversion of DBT was used as measure of the catalytic activity. For comparison purpose, the activity of a conventional industrial $CoMo/Al_2O_3$ catalyst was also measured under the same experimental conditions.

3. Results

3.1. Nitrogen Adsorption−Desorption. The physical adsorption of nitrogen is a valuable technique for determining the textural properties of mesoporous molecular sieves. The nitrogen adsorption isotherms of the supports and catalysts are shown in Figure 1, panels a and b, respectively. The pore structure parameters, such as the specific area (S_{BET}), cumulative pore volume (V_p), pore diameter, and wall thickness (WT) of the Ti-HMS and CoMo/Ti-HMS samples are listed in Table 2. The Ti-free HMS support manifests the highest specific area—990 m^2 g^{-1}. The specific area gradually decreased with the titanium content following the order: HMS > Ti-HMS-80 > Ti-HMS-40 > Ti-HMS-20. The adsorption−desorption isotherms of the HMS and Ti-HMS supports have the shape of the type IV isotherm according to the IUPAC classification,[27] with a sharp step at intermediate relative pressures. The appreciable type H1 hysteresis loops indicate the presence of textural mesopores and cylindrical pores.[28] The adsorption−desorption isotherms are similar to those of hexagonal mesoporous silicate materials reported by other authors.[29,30] Usually, three well-defined stages can be identified: (i) a slow increase in nitrogen uptake at low relative pressures, corresponding to monolayer−multilayer adsorption on the pore walls; (ii) a sharp step at intermediate relative pressures indicative of capillary condensation in mesopores; and (iii) a plateau at high relative pressures associated with multilayer adsorption on the external surface. The HMS and Ti-HMS supports show two capillary condensation steps. The first hysteresis loop for these materials starts at partial pressure of about 0.35−0.40, indicating the presence of framework mesoporosity. The second hysteresis loop starting at partial pressure of about 0.80−0.85 is due to textural interparticle mesoporosity or macroporosity. This clearly indicates that the HMS and Ti-HMS supports exhibit, in addition to the framework-confined porosity (structural porosity), a uniform textural porosity.

(26) Wagner, C. D.; Davis, L. E.; Zeller, M. V.; Taylor, J. A.; Raymond, R. M.; Gale, L. H. *Surf. Interface Anal.* **1981**, *3*, 211.

(27) Khodakov, A. Y.; Griboval-Constant, A.; Bechara, R.; Villain, F. *J. Phys. Chem. B* **2001**, *105*, 9805.

(28) Tanev, T. P.; Pinnavaia, T. J. *Chem. Mater.* **1996**, *8*, 2068.

(29) Mokaia, R.; Jones, W. *J. Catal.* **1997**, *172*, 211.

(30) Pauly, T. R.; Lu, Yu; Pinnavaia, T. J.; Billinger, S. J. L.; Riker, T. P. *J. Am. Chem. Soc.* **1999**, *121*, 8835.

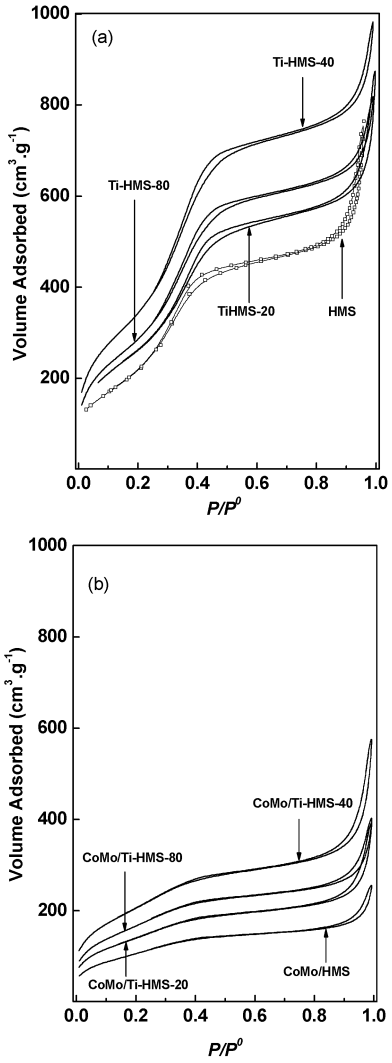

Figure 1. Nitrogen adsorption isotherms of the pure Ti-HMS supports (a) and CoMo/Ti-HMS catalysts (b).

The pore diameter gradually increases in the following order: HMS < Ti-HMS-80 < Ti-HMS-40 < Ti-HMS-20 (Table 2). This trend is consistent with the partial pressure at which, after the filling of the monolayer, a capillary condensation process starts. The capillary pore filling of the HMS support starts at lower pressure than the capillary pore filling in the Ti-HMS supports (Figure 1a), in agreement with the observed pore diameter of the HMS sample. The inflection point at lower partial pressure in the N_2 adsorption−desorption isotherms, and the presence of a single intense reflection at small angles in the X-ray pattern (see below) for the HMS and Ti-HMS supports indicate that both possess regular mesopores.

The adsorption−desorption isotherms of the catalysts also display the shape of the type IV isotherm according to the IUPAC classification (Figure 1b). The corresponding textural properties are summarized in Table 2. The S_{BET} specific area decreases with the deposition of Mo and Co on the supports. The values of S_{BET} follow the order: CoMo/Ti-HMS-40 > CoMo/Ti-HMS-80 > CoMo/Ti-HMS-20 > CoMo/HMS. One can conclude that the effect of Ti is not linear, and at medium concentrations the decrease of the surface area is less than that at high concentrations. The Ti-free CoMo catalyst shows the largest decrease in the surface area among the catalysts studied. Besides, it seems that the Ti ions preserve the surface area values since all Ti-containing catalysts have higher surface areas in comparison to the surface area of the Ti-free catalysts. The observed strong decrease in the specific areas of the CoMo/HMS and CoMo/Ti-HMS-20 samples might indicate that, under the conditions of impregnation and calcination employed in this work, larger CoMo particles are formed on these supports, which block the pores. The pore diameter significantly decreases with the deposition of the active species in the Ti-free sample. Again, one can observe, that the incorporation of Ti preserves the structural properties of the supports and catalysts, since the pore diameter of the Ti-containing catalysts remains practically the same as that of the supports. Besides, this result is an indication of better dispersion of the CoMo phase in the Ti-containing samples in comparison to the Ti-free sample. It can be concluded that the Ti incorporation into the HMS framework favors the preservation of the structural properties of the supports upon deposition of the active phases.

3.2. X-ray Diffraction. The XRD measurements were employed in order to study the mesoporous structure of the supports and catalysts and the crystalline phases of the calcined catalysts. The X-ray diffraction patterns of the Ti-HMS and CoMo/Ti-HMS samples in the 2θ interval between 0.5° and 15° are shown in Figure 2, panels a and b, respectively. An intensive reflection, characteristic of the HMS materials, is observed at about 1.3°. The presence of this small angle peak (d_{100} peak) was first reported by Tanev and Pinnavaia.[18] Gotier and Tuel[25] reported a similar XRD pattern for a Ti-HMS material. Materials exhibiting this single low-angle peak are considered to possess short-range hexagonal symmetry with uniform pore diameter.[30] The d_{100} peak is shifted to lower angles, and an increase in its intensity is observed with the incorporation of Ti, indicating that a lattice expansion, a decrease in the dimensions of the scattering domain, and an increase of the pore diameter occur. The *d*-spacing gradually decreased in the following order: Ti-HMS-20 > Ti-HMS-40 > Ti-HMS-80 > HMS (Table 2). The highest wall thickness was observed for the HMS sample (4.4 nm). The wall thickness decreased in the following order: HMS > Ti-HMS-40 > Ti-HMS-80 > Ti-HMS-20 (Table 2).

Figure 2b shows that the intensity of the reflection peak of the CoMo/HMS sample decreases substantially in comparison to the peaks of the CoMo/Ti-HMS samples. Besides, the bandwidth of this peak increases, and it is shifted to higher angles in comparison both to the peak position in the pure HMS support and to the positions of the peaks of the Ti-containing catalysts. This can be attributed to a partial collapse of the HMS framework during the impregnation and calcination. On the contrary, the peaks of the Ti-HMS supported catalysts remain virtually unchanged upon CoMo deposition in comparison to the peaks of the pure Ti-HMS.

The X-ray diffraction patters of the Ti-HMS and CoMo/Ti-HMS samples in the 2θ interval from 5° to 80° are shown in Figure 3. The X-ray patterns of the supports show a broad line between 20° and 30°, which is attributed to the amorphous part of the substrates. The CoMo/HMS sample

Table 2. Textural Properties of the Ti-HMS Supports and CoMo/Ti-HMS Catalysts

sample	S_{BET} ($m^2\,g^{-1}$)	pore diameter (nm)	pore volume ($cm^3\,g^{-1}$)	d_{100}[a] (nm)	a_0[b] (nm)	wall thickness[c] (nm)	TiO_2[d] (wt %)
HMS	990	3.1	1.32	6.48	7.49	4.39	0.0
Ti-HMS-80	975	3.3	1.32	6.52	7.6	4.3	1.61
Ti-HMS-40	961	3.4	1.74	6.65	7.67	4.27	3.18
Ti-HMS-20	952	3.6	1.37	6.71	7.7	4.1	6.16
CoMo/HMS	432	2.7	0.74	5.5	6.5	3.8	0.0
CoMo/Ti-HMS-80	554	3.4	0.52	6.4	7.4	4.0	1.37
CoMo/Ti-HMS-40	655	3.4	0.99	6.5	7.5	4.1	2.67
CoMo/Ti-HMS-20	534	3.5	0.58	6.5	7.5	4.0	5.27

[a] *d*-spacing is calculated from the X-ray patterns. [b] Unit cell parameter a_0 is calculated by $(2d_{100})/(\sqrt{3})$. [c] Wall thickness is obtained by subtracting pore size from the unit cell parameter. [d] TiO_2 wt % was derived from chemical analysis (atomic absorption).

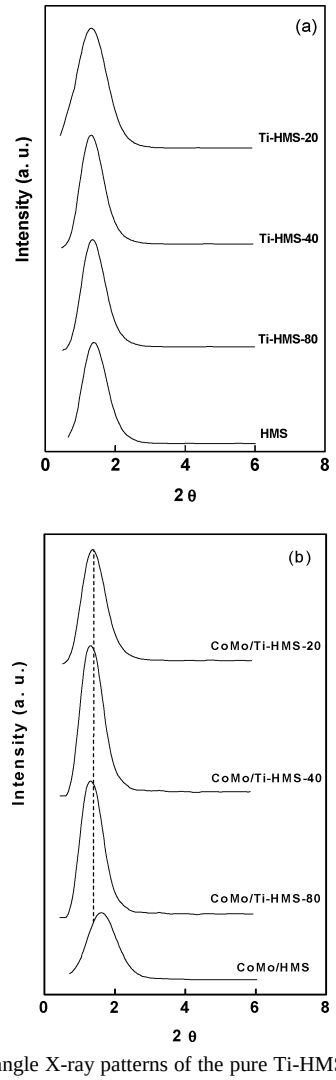

Figure 2. Low-angle X-ray patterns of the pure Ti-HMS supports (a) and calcined CoMo/Ti-HMS catalysts (b).

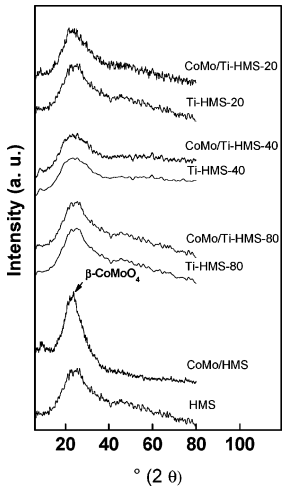

Figure 3. X-ray patterns traces in the 2θ from 5° to 80 ° range of the pure Ti-HMS supports and CoMo/Ti-HMS catalysts.

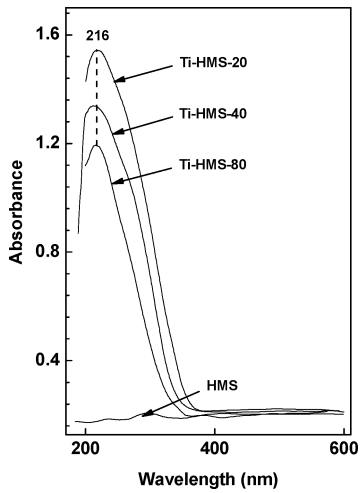

Figure 4. DRS UV−vis spectra of the pure Ti-HMS supports.

exhibited a small peak of β-$CoMoO_4$,[31,32] which overlaps with the broad diffraction of the amorphous part of the support.[23] No reflections belonging to molybdenum and cobalt oxides were observed. One can conclude that the titanium incorporation into the HMS framework results in the formation of highly dispersed CoMo phases and inhibits the formation of the β-$CoMoO_4$ phase.

3.3. UV−Vis Diffuse Reflectance Spectroscopy. UV−vis diffuse reflectance spectroscopy was used to verify the incorporation of the titanium ions into the hexagonal mesoporous silica framework and to determine the symmetry of the Mo and Co species in the CoMo samples. The corresponding electronic spectra of the Ti-HMS materials are shown in the Figure 4. The spectra show an absorption band at 216 nm, which can be attributed to ligand-to-metal charge transfer (LMCT) associated with isolated Ti $^{4+}$ framework sites in tetrahedral coordination.[33,34] The electronic spectrum of HMS did not show, as expected, this LMCT band. In bulk titanium this band is observed in the 320−330 nm range.[35]

(31) Cauzzi, D.; Deltratti, M.; Predieri, G.; Tiripicchio, A.; Kaddouri, A.; Mazzocchia, C.; Tempesti, E.; Armigliato, A.; Vignali, C. *Appl. Catal. A* **1999**, *182*, 125.
(32) Radwan, N. R. E.; Ghozza, A. M.; El-Shobaky, G. A. *Thermochim. Acta* **2003**, *98*, 211.

The electronic spectra of the supports do not contain this band, which suggests that the majority of the Ti ions are [34]incorporated into the silica framework. Additionally we also carried out a Raman study of the support (not shown here). The peak typical for the presence of segregated crystalline TiO_2 anatase phase at about 144 cm^{-1} [36] was not observed, indicating that most of the Ti ions are incorporated into the silica framework.

A number of studies indicate that the shoulder observed at 250−270 nm can be attributed to the presence of Ti ions in pentahedral and octahedral coordination with adsorbed water molecules in the coordination sphere.[37,38] However, the intensive band at 216 nm band clearly indicates that the majority of the Ti ions occupy tetrahedral sites. The slight shift and an increase in the width of this band with increasing of Ti loading may be indicative of the presence of Ti ions in a distorted tetrahedral environment and/or of the presence of Ti species with octahedral or pentahedral coordination.[39] The possibility that some Ti−O−Ti clustering takes place, at high Ti content, cannot be excluded, as it has been observed in mixed TiO_2−SiO_2 gels displaying an absorption band in the 270−330 nm range.[40]

The spectra of the CoMo/HMS and CoMo/Ti-HMS-80 samples are shown in Figure 5a, and these of the CoMo/Ti-HMS-40 and CoMo/Ti-HMS-20 homologues are displayed in Figure 5b. The spectra were fitted by using Gaussian components whose maxima are placed at around 330, 400, 530, 574, and 610 nm for the CoMo/HMS sample (Figure 5a). As the spectra of the other three Ti-containing samples are more complex, the fitting required six instead of five Gaussian components. This sixth component appears at low wavelength (ca. 250 nm). The only allowed band in the UV−vis electronic spectra of the Mo $^{6+}$ ions with d^0 electronic configuration is the ligand−metal charge-transfer band (LMCT) $O^{2-} \rightarrow Mo^{6+}$. The bands at the lower wavelength region (220−270 nm) and that at the higher wavelength region (320−350 nm) according to the literature[41−43] are due to isolated tetrahedral MoO_4^{2-} (Mo_T) and octahedral Mo^{6+} (Mo_O) species, respectively.[41,42] The tetrahedral species of Mo are practically absent in the Ti-free sample. Besides, the decomposition of the peak in the UV region shows that the amount of octahedral Mo species exposed on the surface of Ti-containing samples is larger than that of the Ti-free sample. In the Ti-containing samples the peak is broader, which indicates that small particles of different size and shape are present on the surface. On the contrary, the peak of Ti-free sample is sharp and symmetrical, which reflects the presence of a well-structured phase. As indicated by the XRD patterns, this peak can be assigned to the Mo species in the β-$CoMoO_4$ phase. One can conclude that the dispersion of Mo in the presence of Ti is much higher than that in the Ti-free sample. One should note that in the Ti-free sample no tetrahedral Mo species are observed. It seems that the incorporation of Ti ions in the silica framework enhances the formation of tetrahedral Mo species.

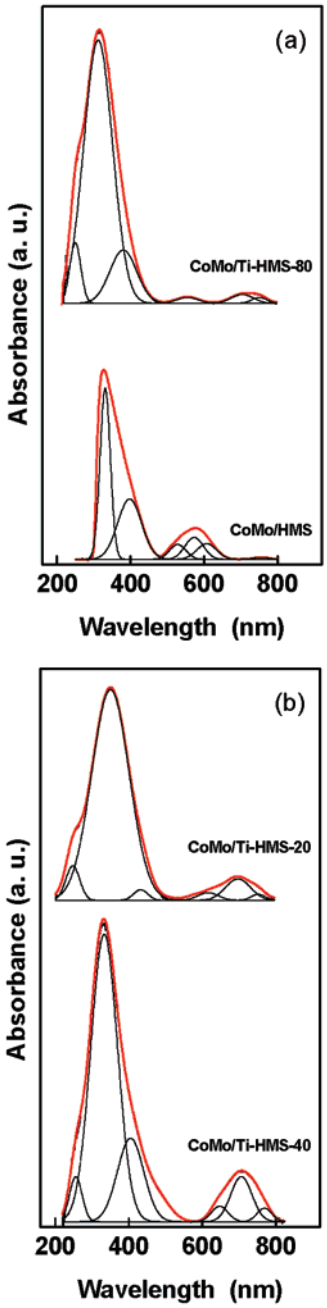

Figure 5. DRS UV−vis spectra of the CoMo/Ti-HMS catalysts and their deconvolution into Gaussian lines: CoMo/HMS and CoMo/Ti-HMS-80 (a); CoMo/Ti-HMS-40 and CoMo/Ti-HMS-20 samples (b).

An absorption band at 395 nm is observed for all catalysts. This band can be attributed to octahedral Co^{2+} species.[44,45]

(33) Zhang, W.; Fröba, M.; Wang, J.; Tanev, P. T.; Wong, J.; Pinnavaia, T. J. *J. Am. Chem. Soc.* **1996**, *118*, 9164.
(34) Klaas, J.; Schulz-Ekloff, G.; Jaeger, N. I. *J. Phys. Chem. B* **1997**, *101*, 1305.
(35) Kosuge, K.; Singh, P. S. *J. Phys. Chem. B* **1999**, *103*, 3563.
(36) Choi, H. C.; Jung, Y. M.; Kim, S. B. *Vib. Spectrosc.* **2005**, *37* (1), 33.
(37) Prakash, A. M.; Sung-Suh, H. M.; Kevan, L. *J. Phys. Chem. B* **1998**, *102*, 85.
(38) Notari, B. *Adv. Catal.* **1996**, *41*, 253.
(39) Geobaldo, F.; Bordiga, S.; Zecchina, A.; Giamello, E.; Leofanti, G.; Petrini, G. *Catal. Lett.* **1992**, *16*, 109.
(40) Anpo, M.; Nakaya, H.; Kodama, S.; Kubokawa, Y. *J. Phys. Chem.* **1986**, *90*, 1633.
(41) Chung, K. S.; Massoth, F. E. *J. Catal.* **1980**, *64*, 320.
(42) Fournier, M.; Louis, C.; Che, M.; Chaquin, P.; Masure, D. *J. Catal.* **1989**, *11*, 400.
(43) Praliaud, H. *J. Less-Common Met.* **1977**, *54*, 387.
(44) Verberckmoes, A. A.; Uytterhoeven, M. C.; Schoonheydt, R. A. *Zeolites* **1997**, *19*, 180.
(45) Papadopoulou, Ch.; Vakros, J.; Matralis, H. K.; Voyiatzis, G. A.; Kordulis, Ch. *J. Colloid Interface Sci.* **2004**, *274*, 159.

On the other hand, we should note that the visible part of the spectrum of the Ti-free catalyst is quite different from that of the Ti-containing catalysts: a broad triple band, centered at about 578 nm is observed. The assignment of this broad band caused some controversy in the literature. Herrera and Resasco[46] assigned this band to octahedral Co species in a $CoMo/SiO_2$ catalyst with a Co/Mo ratio similar to that of our samples. The authors state that this band appears when the Co and Mo species are not in an intimate contact. However, for alumina-supported species, this band was attributed[47,48] to tetrahedrally coordinated Co^{2+} species. At first sight, it seems strange that tetrahedral species might exist on a silica support. However, one should take into account that an interaction between the Co precursor and the support might occur during the calcination of the catalysts, resulting in the formation of Co_2SiO_4 where the Co ions occupy tetrahedral sites. In fact, this reaction readily takes place at temperatures as low as 623 K,[49] which is well below the temperature of calcinations of our samples. The intensity of this band strongly decreases in the Ti-containing catalysts (Figure 5a,b). One can conclude that the presence of Ti inhibits significantly the formation of Co_2SiO_4, which is inactive in the target reaction, since under the employed work conditions it is very difficult to sulfide.

The Ti-containing catalysts also show absorption bands at around 400 and 750 nm, which can be attributed to octahedral Co^{2+}, while the absorption band at approximately 700 nm is usually assigned to octahedral Co^{3+} species.[50,51] On the other hand, the absorption bands around 650 and 610 nm, present in the CoMo/Ti-HMS-40 and CoMo/Ti-HMS-20, can be attributed to small amounts of tetrahedral Co^{2+} species.[51] One can conclude that the amount of octahedral Co^{2+} species exposed on the surface in the Ti-containing samples is much higher than that of the tetrahedral.

3.4. X-ray Photoelectron Spectroscopy. Calcined pure supports and sulfide catalysts were studied byX-ray photoelectron spectroscopy. The Ti 2p core-level spectra of the calcined Ti-HMS supports are shown in Figure 6. The most intensive Ti $2p_{3/2}$ peak of the octahedrally coordinated Ti ions in pure titanium is observed at 458.6 eV. The Ti $2p_{3/2}$ peak in TiO_2-SiO_2 mixed oxides with Ti loadings below 1 wt % appears at 460.1 eV, which is typical of tetrahedrally coordinated titanium.[52] The values of the BE and surface atomic ratios of the Ti-HMS supports are shown in Table 3. The spectrum of the Ti-HMS-80 sample shows only one peak at 460 eV (Figure 4), indicating that practically all Ti ions have been incorporated into the HMS framework. However, the spectra of the Ti-HMS-40 and Ti-HMS-20 samples

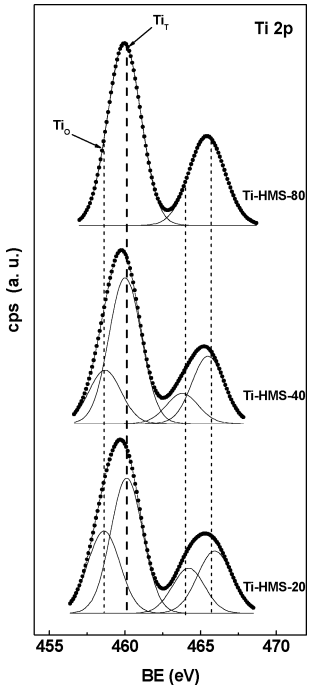

Figure 6. XPS spectra of Ti 2p core levels for pure Ti-HMS supports.

Table 3. Binding Energies (eV) of Core Levels and Surface Atomic Ratios of the Pure Ti-HMS Supports

sample	Si 2p	Ti $2p_{3/2}$	Ti/Si at
HMS	103.4	-	-
Ti-HMS-80	103.4	460.0 (100) 458.6 (22)	0.005
Ti-HMS-40	103.4	460.1 (78) 458.6 (33)	0.008
Ti-HMS-20	103.4	460.1 (67)	0.013

Table 4. Binding Energies (eV) of the CoMo/Ti-HMS Catalysts after Sulfidation at 673 K

sample	Mo $3d_{5/2}$	Co $2p_{3/2}$	% area of Co $2p_{3/2}$ peaks	Ti $2p_{3/2}$	S 2p
CoMo/HMS	228.0	778.2 780.8	51 49	-	161.2
CoMo/Ti-HMS-80	228.0	778.0 780.7	53 47	459.9	161.1
CoMo/Ti-HMS-40	228.1	778.1 780.6	40 60	460.0	161.3
CoMo/Ti-HMS-20	228.0	778.1 780.5	42 58	459.8	161.2

contain not only the intensive peak at 460.1 eV but also a minor one at 458.6 eV, characteristic, as stated above, of titanium ions in octahedral (and/or pentahedral) coordination with water molecules or OH groups included in the coordination sphere. Besides, with the increase of the Ti content, the intensity of the bands of both the octahedral and the tetrahedral species also increases, as could be expected.

The BE values of the Mo $3d_{5/2}$, Co 2p, Ti 2p, and S 2p core levels of the sulfided catalysts are presented in Table 4. All catalysts have the S 2p peak at 161.2 ± 0.1 eV, which is characteristic of S^{2-} ions. The absence of a second component at BE around 168 eV, where sulfate species are usually observed, indicates that the experimental procedure followed during sulfidation and sample transfer within the spectrometer chamber was efficient in avoiding air contact. The Ti $2p_{3/2}$ core level shows a single peak with BE value at 459.8 eV, which is characteristic of titanium ions in

(46) Herrera, J. E.; Resasco, D. E. *J. Catal.* **2004**, *221*, 354.
(47) Hanke, W.; Bienert, R.; Jerchkewitz, H. G. *Z. Anorg. Allg. Chem.* **1975**, *414*, 109.
(48) Matralis, H. K.; Papadopoulou, Ch.; Lycourghiotis, A. *Appl. Catal. A* **1994**, *116*, 221.
(49) Pascal, P. *Nouveau Traité de Chimie Minérale*; Masson: Paris, 1963; Tome XVII, p 354.
(50) Portela, L.; Grange, P.; Delmon, B. *Catal. Rev.—Sci. Eng.* **1995**, *37*, 699.
(51) Kung, M. C.; Kung, H. H. *Catal. Rev.—Sci. Eng.* **1985**, *27*, 425.
(52) Capel-Sánchez, M. C.; Campos-Martín, J. M.; Fierro, J. L. G.; De Frutos, M. P.; Padilla Polo, A. *Chem. Commun.* **2000**, 855.

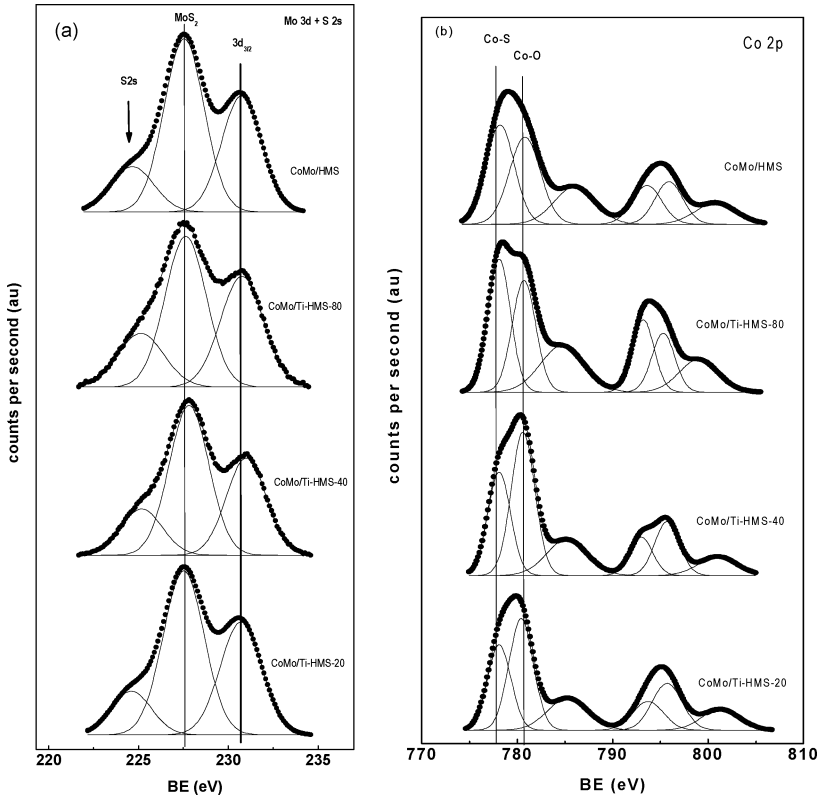

Figure 7. Mo 3d (a) and Co 2p (b) core level spectra of the CoMo/Ti-HMS catalysts after sulfidation at 673 K.

Table 5. Surface Atomic Ratios (from XPS) of the CoMo/Ti-HMS Catalysts after Sulfidation at 673 K

sample	Mo/Si at	Co/Si at	Ti/Si at	Co/Mo at	[Co−S(778.1 eV)]/ [Co−O(780.5 eV)] ratio	S/(Mo + Co) at
CoMo/HMS	0.013	0.0071		0.55	1.11	1.23
CoMo/Ti-HMS-80	0.017	0.0109	0.008	0.64	0.97	1.41
CoMo/Ti-HMS-40	0.019	0.0203	0.011	1.06	0.72	1.34
CoMo/Ti-HMS-20	0.022	0.0207	0.019	0.94	0.81	1.16

tetrahedral (Ti−O−Si) coordination.[53] The same peak (BE ca. 459.8−460.0 eV) was observed in the XP spectra of all oxides (not shown) and sulfided CoMo catalysts (Table 4). This means that all OH groups or water molecules are removed during the sulfidation procedure and only tetrahedrally coordinated Ti ions are detected.

The Mo 3d and Co 2p levels XPS spectra of the sulfided CoMo catalysts are shown in Figure 7, panels a and b, respectively. The Mo $3d_{5/2}$ peak in MoO_3 species is usually observed at 232.6 eV.[54] The Mo 3d spectra of all catalysts show a narrow peak with BE close to that found for pure MoS_2 (228.1 eV).[55] The absence of peaks corresponding to oxy-sulfide species (like $MoO_2S_2^{2-}$) indicates that a complete sulfidation of the molybdenum species has occurred. The Co $2p_{3/2}$ spectra display two contributions: at 778.0−778.2 and at 780.5−780.8 eV corresponding to sulfide Co species[54] and to nonsulfided Co^{2+} species, respectively. The peak at about.779 eV, typical of Co_9S_8,[56] was not observed in our samples. Obviously, the sulfidation of the Co species is incomplete and varies significantly between the different catalysts (as determined from the area ratio of the respective peaks (Table 4)). One can note that the sulfidation of the Co species is the highest for the Ti-free sample followed by the sample with the lowest Ti content. The degree of sulfidation of the sample with intermediate Ti content is the lowest, followed by the sample with the highest Ti content. We should note that the effect of Ti incorporation into the support is not linear and most probably is related to changes in the dispersion of the Co species and in their specific electronic properties. We will return to this point in the discussion of the catalytic activity results. Table 5 compiles the Mo/Si, Co/Si, Ti/Si, and Co/Mo surface atomic ratios of the freshly sulfided catalysts. As expected, the Mo/Si and Ti/Si atomic ratios increased with the increase of the Ti content. The Co/Si atomic ratio also increases with Ti content. Thus, one can conclude that the increase in the Ti content has a favorable effect on the dispersion of the supported metals. However, the degree of sulfidation does not follow the same tendency (Table 5). Obviously, the sulfidation of the Co species is more difficult for the samples with Si/Ti atomic ratio of 40 and 20, although they have

(53) Briggs, D., Seah, M. P., Eds. In *Practical Surface Analysis. Auger and X-ray Photoelectron Spectroscopy*; Wiley: New York, 1990; p 607.

(54) Declerck-Grimee, R. I.; Canesson, P.; Friedman, R. M.; Fripiat, J. J. *J. Phys. Chem.* **1978**, *82* (8), 889.

(55) Okamoto, Y.; Ishihara, S.; Kawano, M.; Satoh, M.; Kubota, T. *J. Catal.* **2003**, *217*, 12.

(56) Schraml-Marth, M. L., Waltehr, K.; Wokaun, A. *J. Non-Cryst. Solids* **1992**, *111*, 143.

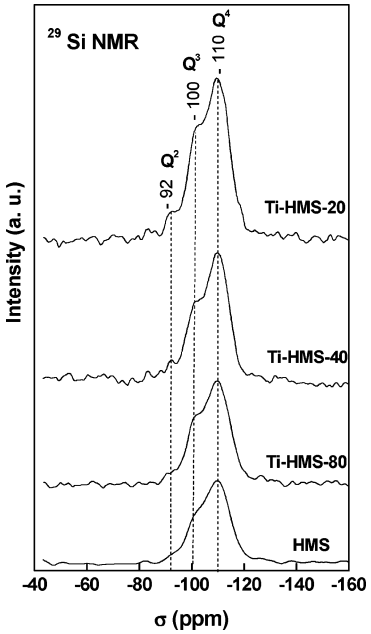

Figure 8. ^{29}Si NMR spectra of the Ti-HMS supports.

higher dispersion. In addition, the sample with the highest dispersion of Co species (Si/Ti at ratio = 20) has a slightly higher degree of sulfidation than the sample with Si/Ti at ratio = 40. Obviously, besides the effect on the dispersion, the concentration of Ti has some specific effect on the electronic properties of the Co species, which results in different sulfidability of the samples. Moreover, the values of the Co/Mo ratio of the samples follow the order CoMo/Ti-HMS-40 > CoMo/Ti-HMS-20 > CoMo/Ti-HMS-80 > CoMo/HMS. This tendency does not coincide with the degree of sulfidation. In light of the above results, different catalytic properties of the samples would be expected.

3.5. ^{29}Si NMR Spectra. The solid state ^{29}Si NMR spectroscopy was used for the study of the Ti ions incorporation into the HMS framework. The NMR spectra of the calcined HMS and Ti-HMS supports are shown in Figure 8. Three peaks: at −92, −100, and at −110 ppm are observed. The peak at −92 ppm corresponds to Q^2 species and the peaks at −100 and −110 were assigned to Q^3 and Q^4 species, respectively.[56] The Q^4 resonance is assigned to silica species (SiO_4). The Q^2 and Q^3 resonances can be assigned to −OH and O−Ti groups bonded to Si, respectively. Zhang et al.[33] compared the spectra of MCM-41 and Ti−MCM-41 and observed a dramatic increase in the amount of Q^4 species. The authors explained this result by the formation of a more cross-linked framework in the presence of Ti ions. Therefore, one could expect that in our samples the value of Q^4 in the Ti containing samples would be higher than that of the Ti free sample. Besides, the signal intensity of the Q^3 species should also increase with the Ti content, if the Ti ions are incorporated into the framework of the HMS material. Indeed, the intensities of the Q^4 species follow the order Ti-HMS-20 > Ti-HMS-40 > Ti-HMS-80 > HMS. The values of the intensities of the Q^2 and Q^3 species follow the same order, as could be expected. However, the relative increase of the Q^2 and Q^3 values is higher than that of the increase of the Q^4 values. As a result, the $Q^4/(Q^2 + Q^3)$ ratio, which could be taken as a measure of the incorporation of the Ti ions into the silica framework, follows the order HMS > Ti-HMS-80 > Ti-HMS-40 > Ti-HMS-20. This result, together with the DRS, Raman, and XPS results indicate that the Ti ions in our samples, indeed, are incorporated into the framework of the HMS material.

3.6. IR of Adsorbed NO. Nitric oxide adsorption is a widely used technique to determine the nature and properties of the exposed ions (Co^{2+}, Mo^{4+}) in hydrotreatment catalysts. The infrared frequencies and the shifts in the position of the stretching vibrations of the adsorbed NO molecule give information about the oxidation state of the metals and their dispersion. One of the important features of the adsorption of this molecule is that it provides independent and simultaneous information on the adsorption sites associated to Mo and Co ions in the oxide state. Freshly calcined Mo catalysts, where molybdenum is as Mo^{6+}, do not adsorb NO.[48] However, if a reducing treatment is performed, then NO molecules adsorb on the reduced sites in the form of dinitrosyl species whose symmetric and asymmetric stretching vibration modes appears at about 1800−1815 and 1700−1715 cm^{-1}, respectively.[50,51,57−60,68−70] The adsorption of nitric oxide on Co^{2+} ions gives rise to a band at about 1800−1880 cm^{-1}, corresponding to the symmetric stretching vibration mode[61−66] and to another one at about 1750−1800 cm^{-1}, corresponding to the asymmetric stretching vibration mode.[51,67] This means that when both Co^{2+} and reduced $Mo^{\delta+}$ ($5 \geq \delta \geq 4$) ions are present, the antisymmetric vibration mode of NO adsorbed on Co^{2+} overlaps with the symmetric vibration mode of NO adsorbed on $Mo^{\delta+}$ and hence three instead of four bands would be observed.

The decomposition into Gaussian lines of the IR spectra of NO adsorbed on the CoMo/HMS and CoMo/Ti-HMS samples are presented in Figure 9. The strong doublet observed at about 1889 and 1807 cm^{-1} (symmetric and asymmetric stretching vibrations, respectively) is indicative of the presence of Co^{2+} ions on the surface. The presence of a small amount of partially reduced $Mo^{\delta+}$ species, generated upon degassing of the samples under high vacuum, is evidenced by the appearance of a low intensity doublet at about 1788 and 1700 cm^{-1}, corresponding to the symmetric and asymmetric stretching vibrations of a dinitrosyl species adsorbed on $Mo^{\delta+}$ sites.

(57) Peri, J. B. *J. Phys. Chem.* **1982**, *86*, 1615.
(58) O'Young, C. L.; Yang, C. H.; De Canio, S. J.; Patel, M. S.; Storm, D. A. *J. Catal.* **1988**, *113*, 307.
(59) Segawa, K. I.; Hall, W. K. *J. Catal.* **1982**, *77*, 221.
(60) Valyon, J.; Hall, W. K. *J. Catal.* **1983**, *84*, 216.
(61) Valyon, J.; Schneider, R. L.; Hall, W. K. *J. Catal.* **1984**, *85*, 277.
(62) Okamoto, Y.; Katoh, Y.; Mori, Y.; Imanaka, T.; Teranishi, S. *J. Catal.* **1981**, *70*, 445.
(63) Topsøe, N. Y.; Topsøe, H. *J. Catal.* **1982**, *75*, 354
(64) Topsøe, N. Y.; Topsøe, H. *J. Catal.* **1983**, *84*, 386.
(65) Ramírez, J.; Contreras, R.; Castillo, P.; Klimova, T.; Zárate, R.; Luna, R. *Appl. Catal. A* **2000**, *197*, 69.
(66) Ramírez, J.; Cuevas, R.; López Agudo, A.; Fierro, J. L. G. *Appl. Catal.* **1990**, *57*, 223.
(67) Yao, H. C.; Shelef, M. *J. Phys. Chem.* **1974**, *78*, 240.
(68) Prada Silvy, R.; Beuken, J. M.; Fierro, J. L. G.; Bertrand, P.; Delmon, B. *Surf. Interface Anal.* **1986**, *8*, 167.
(69) Cáceres, C.; Fierro, J. L. G.; López Agudo, A.; Severino, F.; Laine, J. *J. Catal.* **1986**, *97*, 219.
(70) Okamoto, Y.; Maezawa, A.; Imanaka, T. *J. Catal.* **1989**, *120*, 29.

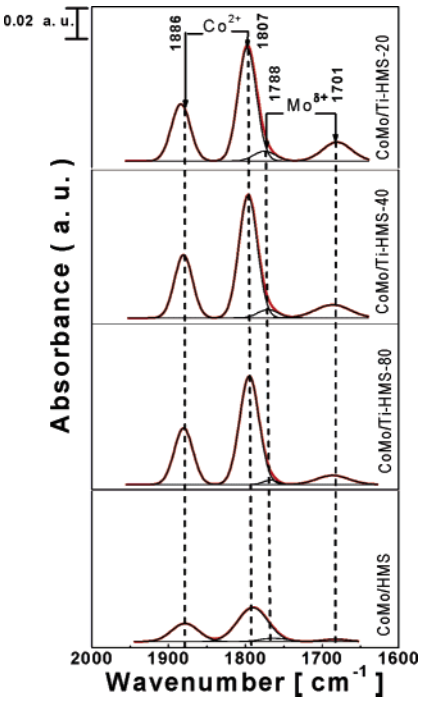

Figure 9. IR spectra of NO adsorbed on the calcined CoMo/Ti-HMS catalysts.

The band around 1887 cm^{-1}, observed for the CoMo/HMS and CoMo/Ti-HMS-80 samples, is slightly shifted to higher wavenumbers upon increasing the titanium content in the support. It appears at 1889 cm^{-1} for the CoMo/Ti-HMS-40 sample and at 1892 cm^{-1} for the CoMo/Ti-HMS-20 sample. This can be due to changes in the environment of the Co species, to which NO is adsorbed.[61]

Additionally, changes of the band intensities of the adsorbed NO on both Mo and Co are observed with the increase of the Ti content. All Ti-containing samples have higher surface areas of adsorbed NO as compared to the surface area of the peak of NO adsorbed on the Ti free sample. The following order is observed for the surface area of the symmetric vibration peak of NO adsorbed on Co species: CoMo/Ti-HMS-40 > CoMo/Ti-20 > CoMo/Ti-HMS-80 > CoMo/HMS. We should note that this order coincides with the order observed for the Co/Mo ratio obtained by XPS and DRS. Again the effect of the Ti content on the increase of the NO adsorption on the Co species is not linear. The order of the surface areas of the symmetric vibration of NO adsorbed on Mo species is the following: CoMo/Ti-HMS-20 > CoMo/Ti-HMS-40 > CoMo/Ti-HMS-80 > CoMo/HMS. This order coincides with the Mo/Si ratio obtained by XPS. This increase in the surface areas of the adsorbed NO with the Ti loading can be attributed to a significant increase in the dispersion of the Co and Mo species or to the formation of new NO adsorbing Co and Mo species at the expense of nonadsorbing ones, in agreement with the XPS and DRS results.

3.7. Catalytic Activity. The degree of conversion of DBT was used as a measure of the catalytic activity. Figure 10 presents the percentage of DBT conversion over the CoMo/Ti-HMS catalysts at $T = 593$ K, $P = 5.5$ MPa, and 6 h of reaction time. For comparison, the performance of a commercial $CoMo/Al_2O_3$ is included. The Ti-free catalyst

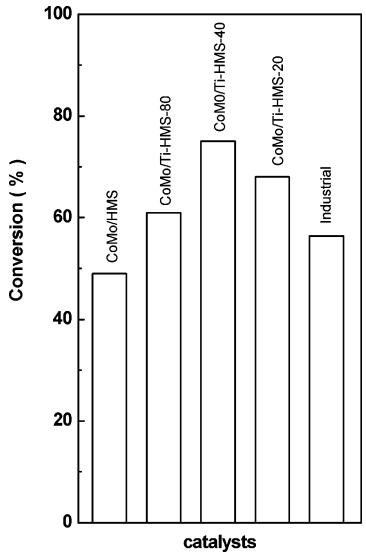

Figure 10. DBT HDS over CoMo/Ti-HMS catalysts at 6 h of reaction time, $T = 593$ K and $P = 5.5$ MPa. Industrial catalyst is used as reference.

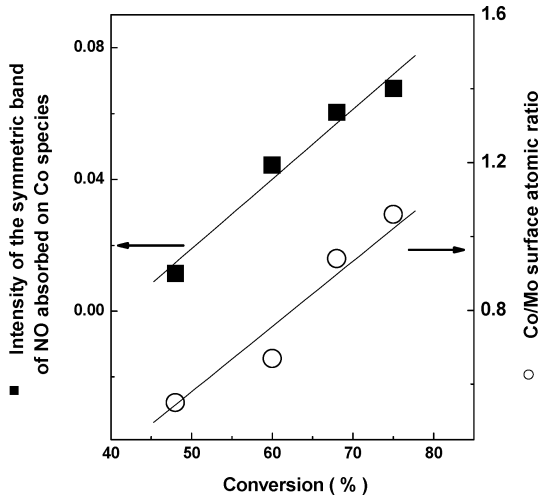

Figure 11. Correlation between DBT conversion over CoMo/Ti-HMS catalysts and intensity of the band of NO adsorbed on oxide Co species (from FTIR−NO of calcined catalysts) and the Co/Mo atomic ratio of sulfided catalysts (from XPS).

(CoMo/HMS) manifests the lowest catalytic activity. The catalytic activity of the samples significantly increases in the Ti-containing catalysts, for which the highest activity is observed on the CoMo/Ti-HMS-40 one. Besides, all Ti-containing samples exhibit higher activity than the commercial CoMo-alumina catalyst. It can be noted that the CoMo/Ti-HMS-40 catalyst is 30% more active than the commercial one and 50% more active than the Ti-free counterpart. Figure 11 shows the dependence of the degree of conversion of DBT on the intensity of symmetric vibration band of NO adsorbed on Co species (from FTIR−NO) and on the Co/Mo ratio, as determined by XPS. This dependence is rather interesting because the CoMo/Ti-HMS-20 sample, which has the highest Mo/Si and Co/Si ratio is not the most active one. While the total amount of Mo species is sulfided in all catalysts, the Co species in the most active sample (CoMo/Ti-HMS-40) are the less sulfided among all other catalysts ((Co−S)/(Co−O) in Table 5) and a linear dependence between the degree of conversion and in the sulfide/oxidized Co species is also observed. We should also note

Table 6. Product Distribution[a] for HDS of DBT over CoMo/Ti-HMS and Industrial Catalysts

	DDS route	HYD route			
catalyst	BP (%)	CHB (%)	DCH (%)	DBT (%)	HYD/DDS[b] ratio
CoMo/HMS	46.55	1.37	0.0	52.0	0.030
CoMo/Ti-HMS-80	58.0	2.85	0.0	39.1	0.050
CoMo/Ti-HMS-40	68.49	5.47	1.0	25.0	0.095
CoMo/Ti-HMS-20	58.38	7.81	1.76	32.0	0.164
industrial	53.46	4.19	0.0	42.3	0.079

[a] The reaction conditions were $T = 593$ K; $P = 5.5$ MPa; 6 h of reaction time. [b] Direct desulfurization is denoted as DDS. Hydrogenation pathway is denoted as HYD. The HYD/DDS ratio is calculated from selectivity of the products [(CHB + DCH)/BP].

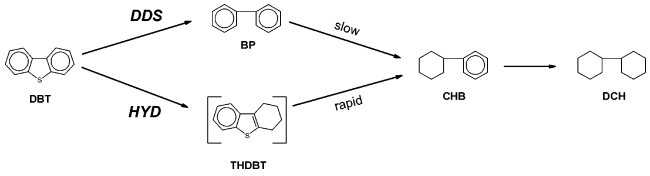

Figure 12. Reaction scheme for the hydrodesulfurization of dibenzothiophene over the CoMo/Ti-HMS and industrial catalysts. The reaction conditions were $T = 593$ K; $P = 5.5$ MPa; 6 h of reaction time.

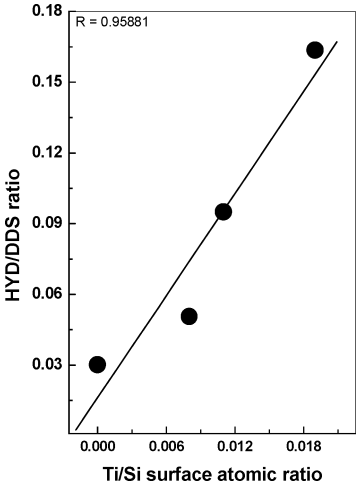

Figure 13. Influence of the Ti content (expressed as Ti/Si surface atomic ratio and determined by XPS of sulfided catalysts) on the reaction pathways (expressed as HYD/DDS ratio) for the hydrodesulfurization of dibenzothiophene over the CoMo/HMS and CoMo/Ti-HMS catalysts. Reaction conditions were $T = 593$ K, $P = 5.5$ MPa, and 6 h of reaction time.

that it seems that at a certain Ti content, to which a specific degree of dispersion of the Co species and of their electronic/chemical properties corresponds, the sulfidation process is limited to the surface Co ions and no propagation in the bulk of the Co particles takes place. Besides, the most active catalyst manifests the highest XPS Co/Mo value, these results imply that not just the dispersion of the active species and their reducibility/sulfidability are responsible for the catalytic activity, but a specific low state of sulfidation of the Co species with specific electronic properties due to the presence of oxidized Co ions in the bulk of the partially sulfided supported Co particles and a specific ratio between the exposed Co and Mo species should exit in order to obtain higher activity. A similar dependence of the catalytic activity on the degree of sulfidation/oxidation of the Co species has been observed by Declerck-Grimee et al.[71]

The product distribution of the catalysts is shown in Table 6. According to the literature,[72] the HDS of DBT proceeds via two major routes, as shown in Figure 12. The possible reaction pathways are as follows: (i) direct desulfurization (DDS) route, which involves the hydrogenolysis of C−S bonds with no hydrogenation of aromatics ring, and (ii) hydrogenation (HYD) route, which requires ring saturation prior to the desulfurization step. In this study, the detected products were BP, CHB, and DCH. The intermediate tetrahydrodibenzothiophene (THDBT), as product of the HYD reaction pathway, was not detected. The main reaction products on the CoMo/HMS and CoMo/Ti-HMS-80 and the commercial catalysts are cyclohexylbenzene (CHB) and biphenyl (BP), while for the CoMo/Ti-HMS-40 and CoMo/Ti-HMS-20 catalysts CHB, BP, and dicyclohexyl (DCH) are the main products. The results in Table 6 clearly indicate that the principal route of the reaction is the direct desulfurization. However, with the increase of Ti content the hydrogenation route also contributes to the total conversion. The CoMo/Ti-HMS-20 catalyst, with the highest Ti loading, shows a superior hydrogenation capability in comparison to the other members of the series, but its contribution to the DDS route is less than that of the most active catalyst. The (CHB + DCH)/BP ratio, which describes the ratio between the routes (HYD/DDS), follows the order: CoMo/Ti-HMS-20 > CoMo/Ti-HMS-40 > CoMo/Ti-HMS-80 > CoMo/HMS. A linear correlation between the Ti/Si atomic ratio and the HDS of DBT via the hydrogenation pathway exists (Figure 13). This result clearly indicates that the presence of Ti in the catalysts promotes the HYD route of DBT HDS, thus contributing to the total conversion of DBT. This effect can be attributed to the structure and specific electronic properties of the active phases formed on the Ti-loaded support.

4. Conclusions

The introduction of Ti ions into the framework of the mesoporous HMS material up to a Si/Ti = 20 (atom ratio) results in complete incorporation of the Ti ions, and no formation of TiO_2 crystallites is detected. The results demonstrate that Ti preserves the framework structure of the HMS material, without significant changes in its specific area, but a significant increase in the pore diameter and the pore volume is observed with the increase of the Ti content. Incorporation of Ti leads to significant changes in both the chemical and catalytic properties of the catalysts. The presence of Ti inhibits the formation of the catalytically inactive Co_2SiO_4 and β-$CoMoO_4$ phases, which are very difficult to sulfide under the conditions employed in this work. The effect of the Ti concentration is not linear. The highest Co/Mo surface ratio in the sulfided catalysts and the largest amount of adsorbed NO on Co species are observed on the CoMo/Ti-HMS-40 catalyst. This catalyst displays the highest activity but is also characterized by the lowest degree of sulfidation of the Co species. It seems that not just a high

(71) Declerck-Grimee, R. I.; Canesson, P.; Frideman, R. M.; Fripiat, J. J. *J. Phys. Chem.* **1989**, *82*, 889.
(72) Kim, H.; Lee, J. J.; Koh, J. H.; Moon, S. H. *Appl. Catal. B* **2004**, *50*, 17.

dispersion and good sulfidation degree of the active species are the conditions to observe high catalytic activity, but a specific degree of oxidation/sulfidation of the promoter, characterized by specific electronic properties of the exposed sulfided Co ions, and a high Co/Mo ratio are necessary to achieve higher activity. All Ti-containing catalysts exhibit higher activity than the industrial alumina-supported CoMo catalyst. The presence of Ti also promotes the hydrogenation route in the reaction of HDS of DBT, but the prevailing route in all catalysts is the DDS one.

Acknowledgment. The authors thank M. Hernández-Landaverde (CINVESTAV-Qro. México) and M. Aguilar Franco (IFUNAM-México) for technical assistance. T.A.Z. expresses his gratitude to CONACyT and DGEP-UNAM, Mexico for financial support. The financial support of DGAPA, UNAM, México, is gratefully acknowledged. The Spanish Ministry of Science and Technology is also acknowledged for funding the PPQ2002-11841-E project.

CM0500051